24th INTERNATIONAL CONGRESS ON SOUND AND VIBRATION
23–27 July 2017, London

# BASIC RESEARCH ON HOT JUDDER OF CAR DISC BRAKES FROM THE VIEWPOINT OF SELF-EXCITED VIBRATION WITH TIME DELAY

Takahashi Kohei

*Oita University, Graduate School of Engineering*
*Email: v16e1017@oita-u.ac.jp*

Nakae Takashi and Ryu Takahiro
*Oita University, Faculty of Engineering, Department of Mechanical and Energy Systems Engineering*

In high-speed areas of highways and roads with steep descents, the heat in car disc brakes sometimes causes a vibration problem. This phenomenon, called hot judder, is generated by hot spots on the surface of the disc. The generation mechanism of hot judder has not yet been clarified. In this study, hot judder is modeled as self-excited vibration due to the time delay caused by heat deformation of the disc, and the fundamental generation mechanism of hot judder is analyzed by a simple three-degree-of-freedom system.

In the analysis, the temperature of the disc is calculated by the difference method. Then, the relations between disc temperature and the expansion due to heat and the shrinkage due to cooling is examined.

It was found that (1) hot judder is an unstable vibration due to the time delay of the fluctuation of brake disc thickness caused by thermal deformation, and (2) the number of hot spots is related to the natural frequency of the system and the rotation speed of the disc.
Keywords: Disc brake, Self-excited vibration, Time delay system, Pattern formation, Judder

## 1. Introduction

In recent years, the competitiveness among automobile manufacturers has prompted the development of quiet and comfortable cars. In particular, vibration, called hot judder, occurs frequently in car disc brakes when braking in high-speed areas of highways and roads with steep descents. Although investigations to reduce squeal and hot judder of car disc brakes have been carried out, these problems still need to be solved. When hot judder occurs, multiple hot spots are generated on the surface of the disc brake. However, the generation mechanism and the countermeasure of hot judder have not yet been found. A previous study [1] reported that the hot spots on the surface of disc brakes are caused by frictional heat with repeated braking. Another study [2] also reported that hot judder is generated by buckling of the disc due to thermoelastic instabilities (TEI). However, these studies did not discuss the vibration mechanism and methods to quantify the number of hot spots. In the present study, the disc brake system is modeled by a simple three-degree-of-freedom system, and the generation mechanism of hot judder is analyzed as self-excited vibration due to the time delay caused by heat deformation of the disc. And calculations of the temperature of the disc by the difference method are described. Then, the relations between disc temperature and the expansion due to heat and the shrinkage due to cooling is examined.

## 2. Temperature calculation model of the disc

The temperature calculation model is shown in Fig. 1(a). The contact width of the brake pad in the

circumferential direction is assumed to be a point on the disc. To consider the distribution of the disc temperature, the disc is modeled by $n$ discrete elements in thickness direction $z$ of the disc, as shown Fig. 1(b). The temperature $T_i^t$ of the $i^{th}$ element at time $t$ for each element is calculated. In Fig. 1(b), dummy points, which are the $0^{th}$ to $n^{th}$ elements at both outside disc surfaces, are assumed in order to calculate the temperature by using the heat flux quantity.

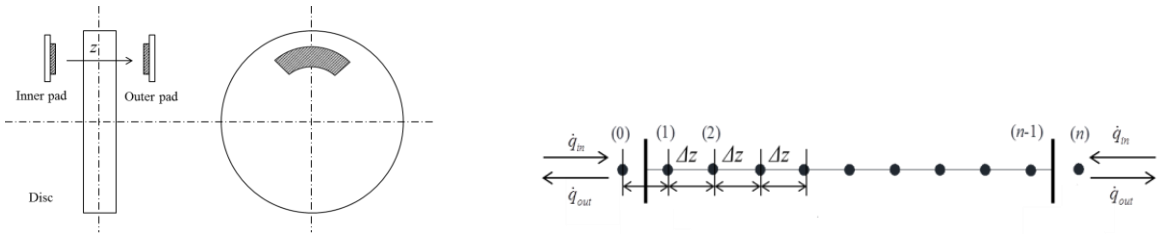


(a) Disc model for thickness direction (b) Discrete points of the thickness

Fig. 1 Temperature calculation model

The assumptions for calculating the temperature of the disc are as follows:

(1) The heat transfer to a pad is omitted.
(2) The ventilated disc rotor is assumed as a solid disc.
(3) The heat transfer is only in the thickness direction, and the heat transfer in the radial and the circumferential directions is neglected.
(4) The circumferential length of the pad contact part for heating is 1/6 of the length of the disc circumference.
(5) The temperature of the $i^{th}$ element at time $t$ is $T_i^t$.
(6) As an initial condition, the temperature of the disc is set at $T_i^0 = 293$ K ($i$=0–$n$) in time $t$=0 s.

## 2.1 Surface temperature calculation of the disc

The heating part of the disc brake is the contact part between the disc and the pad, and the part without any contact is the cooling part. The heat flux quantity per unit area at heating part $\dot{q}_{in}$ and the loss heat flux quantity in cooling part $\dot{q}_{out}$ are given by the Fourier law of heat transfer shown in Eq. (1) [3]. In this study, $\lambda$ is the thermal conductivity of cast iron. $dT/dz$ is negative value at heating part and is positive value at cooling part. The power which is obtained by the frictional force $\mu F$ acting on the rotating disc surface at slipping velocity $r\omega$ in pad contact area is described as $\mu Fr\omega$. The heat flux quantity per unit area at heating part $\dot{q}_{in}$ is shown in Eq. (2). In Eq. (2), the coefficient of friction $\mu$, pad contact pressure $F$, disc radius $r$, disc angular velocity $\omega$, and pad area $A$. For the cooling of the disc, the loss of the quantity of heat flux $\dot{q}_{out}$ in Eq. (1) can be calculated by summation of the quantity of heat flux of the disc and the quantity of heat flux by radiation.

$$\dot{q}_{in} = \dot{q}_{out} = -\lambda \frac{dT}{dz}. \tag{1}$$

$$\dot{q}_{in} = \frac{\mu F r \omega}{A}. \tag{2}$$

Then, the temperature of the disc in the thickness direction is calculated by the one-dimensional unsteady heat equation shown in Eq. (3), where $\kappa$ is the thermal diffusion rate, which is a function of thermal conductivity $\lambda$ of cast iron, specific heat $c$, and density $\rho$, as shown in Eq. (4) [4]. Although the values of $\lambda$ and $c$ vary according to the temperature, the values at 800 K are used as constants in this calculation.

$$\frac{\partial T}{\partial t} = \kappa \frac{\partial^2 T}{\partial z^2}. \tag{3}$$

$$\kappa = \frac{\lambda}{c\rho}. \tag{4}$$

Equation (5) is the discretized equation of Eq. (3). The temperature of the $i^{\text{th}}$ element $T_i^t$ in the disc is calculated by Eqs. (5) and (6).

$$T_i^{t+1} = T_i^t + \frac{\kappa \Delta t}{\Delta z^2}\left(T_{i+1}^t - 2T_i^t + T_{i-1}^t\right) (i=0\sim n). \tag{5}$$

$$\Delta t \le \frac{\Delta z^2}{2\kappa}. \tag{6}$$

In Eq. (5), $\Delta t$ is an interval of time and is needed to satisfy Eq. (6) because the time variation of the temperature cannot be calculated precisely when the interval of time $\Delta t$ is greater than the time of the diffusion of heat for each element.

## 2.2 Numerical computation result

The parameters for the calculations are shown in Table 1 [5]. Figure 2 shows the result of the disc temperature calculation of inner side surface $T_1^t$. The abscissa shows time $t$ and the ordinate shows temperature $T_1^t$. In Fig. 2, two processes, one for the temperature increase and the other for the decrease, are shown. In addition, the disc thickness with the temperature increase is calculated from Eqs. (7) and (8). The material is assumed to be cast iron.

Table 1 Values of parameters for calculation of the temperature model

| | | | | | |
|---|---|---|---|---|---|
| $\mu$ | 0.3 | $v_0$ | $65.09\times10^{-6}$ m$^2$/s | $\omega$ | 251 rad/s |
| $F$ | $2.83\times10^{3}$ N | $f(Pr,n)$ | 0.330 | $T_w$ | 1073 K |
| $r$ | 0.2 m | $\varepsilon$ | 0.2 | $a$ | $11\times10^{-6}$ 1/℃ |
| $\lambda$ | 31.4 W/(m · K) | $H$ | 0.028 m | $\lambda_0$ | $50.33\times10^{-3}$ W/(m · K) |
| $\rho$ | 7180 kg/ m$^3$ | $n$ | 221 | $\sigma$ | $5.67\times10^{-8}$ W/(m$^2$ · K) |
| $T_\infty$ | 293 K | $\kappa$ | $6.30\times10^{-6}$ m$^2$/s | | |
| $A$ | $41.73\times10^{-4}$ m$^2$ | $c$ | 0.695 kJ/(kg · K) | | |

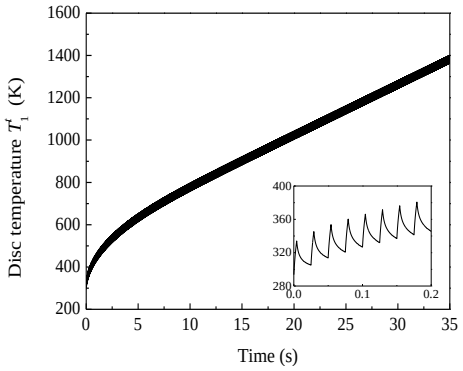


Fig. 2 Temperature of disc surface over time

$$T_{ave} = \frac{\left(\sum_{1}^{n-1} T_i\right)}{n-1}. \tag{7}$$

$$H' = (T_{ave} - 293) \times H \times a + H \,. \tag{8}$$

Figure 3 shows the average values of the disc temperature. Figure 4 shows the variation of the disc thickness. As a result of Figs. 2 to 4, it is confirmed that the effect of air-cooling of the disc is small because the loss of heat flux quantity $\dot{q}_{out}$ in the cooling part is small. Specifically, the loss is 0.397% of heat flux quantity $\dot{q}_{in}$ in the heating part when the angular velocity $\omega$ is 251 rad/s. Therefore, it is supposed that the effect of cooling is small.

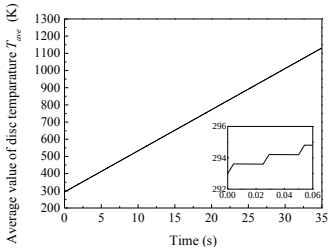


Fig. 3 Average temperature of the disc

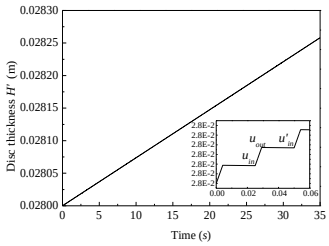


Fig. 4 Disc thickness with thermal expansion

### 2.3 Coefficient of expansion and shrinkage rate of the disc

The expansion rate by the frictional heat of pad $\alpha$ and the shrinkage rate by air-cooling $\beta$ are expressed as Eq. (9).

$$\alpha = \frac{u_{out}}{u_{in}}, \beta = \frac{u'_{in}}{u_{out}} \,. \tag{9}$$

Here, $u_{in}$ and $u_{out}$ are the disc thicknesses just before the disc enters the contact area with the pad at the leading edge, and just after the disc passes through the contact area with the pad at the trailing edge, respectively. In addition, $u'_{in}$ is the disc thickness of $u_{in}$ after one disc rotation period $T$. The expansion rate $\alpha$ and the shrinkage rate $\beta$ are approximately 1 for all rotation speeds of the disc. At all rotation speeds of the disc, $\alpha$ and $\beta$ must always satisfy the conditions of $\alpha > 1$ and $\beta < 1$, respectively.

## 3. Analysis model

In this section, the disc brake of automobiles is modeled to analyze the fundamental mechanism of hot judder. Hot judder is treated as a self-excited vibration system with a time delay caused by heat. The relations between the number of disc revolutions and the expansion rate by the frictional heat of pad $\alpha$ and the shrinkage rate by air-cooling $\beta$, which were obtained in Section 2.3, are used. In the analysis, the feedback effect of the quantity of thermal expansion is considered.

### 3.1 Analysis model and equation of motion

An analysis model of a three-degree-of-freedom system is shown in Fig. 5. The analysis model consists of a disc, pad, and caliper. The caliper is modeled by inner and outer rigid body blocks, which can vibrate in the bouncing mode in the out-of-plane directions $x_1$ and $x_2$. The out-of-plane displacement of the disc is $x_3$. Pads on the inner and the outer sides are modeled by contact points that have stiffness and damping. The quantities of disc expansion on the inner side and the outer side immediately after the pad exits are defined as $u_i(t)$ and $u_o(t)$, respectively. These quantities of expansion are fed back as forced displacement $\beta u_i(t\text{-}T)$ and $\beta u_o(t\text{-}T)$ on the contact surface after one rotation of the disc (after rotation period $T$ seconds). In other words, this analysis model with the expansion is treated as a time delay system. In addition, the mass of the caliper on the inner side, the mass on the outer side, and the mass of the disc are represented by $m_1$, $m_2$, and $m_3$, respectively. The spring constants

and the damping coefficients are represented by $k_1$, $k_2$, $k_3$, $k_i$, $k_o$, and $c_1$, $c_2$, $c_3$, $c_i$, $c_o$, respectively. Also, $v$ is the thermal expansion displacement per unit frictional force in one rotation of the disc and is assumed to be constant. The equations of motion and thermal expansion immediately after the pad exits can be expressed as follows.

$$m_1\ddot{x}_1 + c_1\dot{x}_1 + k_1x_1 + c_i\{\dot{x}_1 - \dot{x}_3 - \beta\dot{u}_i(t-T)\} + k_i\{x_1 - x_3 - \beta u_i(t-T)\} + c_2(\dot{x}_1 - \dot{x}_2) + k_2(x_1 - x_2) = 0. \quad (10)$$

$$m_2\ddot{x}_2 + c_o\{\dot{x}_2 - \dot{x}_3 + \beta\dot{u}_o(t-T)\} + k_o\{x_2 - x_3 + \beta u_o(t-T)\} + c_2(\dot{x}_2 - \dot{x}_1) + k_2(x_2 - x_1) = 0. \quad (11)$$

$$\begin{aligned} m_3\ddot{x}_3 + c_3\dot{x}_3 + k_3x_3 + c_i\{\dot{x}_3 - \dot{x}_1 + \beta\dot{u}_i(t-T)\} + k_i\{x_3 - x_1 + \beta u_i(t-T)\} \\ + c_o\{\dot{x}_3 - \dot{x}_2 - \beta\dot{u}_o(t-T)\} + k_o\{x_3 - x_2 - \beta u_o(t-T)\} = 0 \end{aligned}. \quad (12)$$

$$u_i(t) = \beta u_i(t-T) - \alpha v[c_i\{\dot{x}_1 - \dot{x}_3 - \beta\dot{u}_i(t-T)\} + k_i\{x_1 - x_3 - \beta u_i(t-T)\}]. \quad (13)$$

$$u_o(t) = \beta u_o(t-T) + \alpha v[c_o\{\dot{x}_2 - \dot{x}_3 + \beta\dot{u}_o(t-T)\} + k_o\{x_2 - x_3 + \beta u_o(t-T)\}]. \quad (14)$$

Variable transformation $\tau = \omega t$, $\omega = 2\pi/T$, and the Laplace transform are applied to these equations. Then, by assuming the coefficient matrix of obtained equation $\boldsymbol{A}$, the characteristic equation can be expressed as follows.

$$\det \boldsymbol{A} = 0. \quad (15)$$

The characteristic value satisfying characteristic Eq. (15) can be expressed $s=\sigma+iN$. The solution is positive infinity. If a root has a positive real part, then hot judder occurs. The imaginary part $N$ of the root corresponds to the number of hot spots.

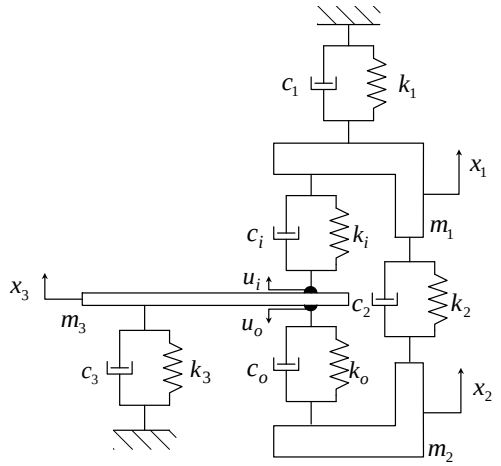

Fig. 5 Analysis model of the disc and caliper

Table 2 Values of parameters of the analysis model

| | | | |
|---|---|---|---|
| $m_1$ | 2.2 kg | $c_i$ | 53.9 Ns/m |
| $m_2$ | 0.22 kg | $c_o$ | 53.9 Ns/m |
| $m_3$ | 58.4 kg | $\zeta_1$ | 0.06369 |
| $k_1$ | $1.9\times10^6$ N/m | $\zeta_2$ | 0.01 |
| $k_2$ | $3.6\times10^7$ N/m | $\zeta_3$ | 0.039 |
| $k_3$ | $1.81\times10^8$ N/m | $v$ | $9.34\times10^{-10}$ m/Nrev |
| $k_i$ | $6.62\times10^6$ N/m | $f_n$ | 400 Hz |
| $k_o$ | $6.62\times10^6$ N/m | $f_1$ | 140 Hz |
| $c_1$ | 273.8 Ns/m | $f_2$ | 2135 Hz |
| $c_2$ | 114.8 Ns/m | $f_3$ | 280 Hz |
| $c_3$ | 8019 Ns/m | | |

## 3.2 Calculation parameter

The parameters for calculation of the analysis model are shown in Table 2. Spring constant $k_1$ represents the stiffness of the support of the caliper and spring constant $k_2$ represents the stiffness of the connection part between the inner and outer sides of the caliper. To determine spring constants $k_1$ and $k_2$, a hammering test on an actual caliper was conducted to measure the first and second natural frequencies $f_1$ and $f_2$, respectively. In addition, the damping ratios of the first and second modes of the caliper were calculated to determine the damping coefficients $c_1$ and $c_2$. Spring constant $k_3$ and damping coefficient $c_3$ represent the stiffness and damping of the disc, respectively. The values of $k_3$ and $c_3$ are determined by measuring the natural frequency $f_3$ and the damping ratio of the (1,0) mode of the disc by the hammering test. Table 3 shows the natural frequencies and natural modes of the system. In the first mode, the caliper and the disc are in phase. In the second mode, the caliper and the disc are out of phase. The contact spring constants $k_i$, $k_o$ between the caliper and the disc are set so that the second frequency of system $f_n$ becomes 400 Hz. The damping coefficients $c_i$, $c_o$ are 0.01, as determined by setting the damping ratio $\zeta_2 = c_{i,o} / 2\sqrt{(m_1 + m_2)k_{i,o}}$.

Table 3 Natural frequencies and natural modes

| Mode | | 1st mode | 2nd mode |
|---|---|---|---|
| Natural frequency | | 273 Hz | 400 Hz |
| Natural mode | $x_1$ | 1.0 | 1.0 |
| | $x_2$ | 0.9495 | 0.8620 |
| | $x_3$ | 0.5822 | -0.07 |

### 3.3 Numerical calculation result

Figure 6 shows the relation between $\sigma\omega$ and the rotation speed of the disc. In this figure, $\sigma\omega$ represents the growth speed of the disc thermal deformation, and $n$ represents the nearest integer of the imaginary part of the characteristic root and is equal to the number of hot spots. If the real part of the characteristic value is positive, then the system is unstable and hot judder occurs; if all the real parts of the characteristic roots are negative, then the system is stable.

In addition, from Fig. 6, the range of rotation speed is confirmed to become unstable for different numbers of hot spots. The peak of $\sigma\omega$ is located at a different rotation speed for each number of hot spots. The relation between the generation frequency of hot judder, the rotation speed of the disc, and the number of hot spots satisfies the equation of (generation frequency of hot judder) = (rotation speed of disc) × (number of hot spots) ≅ (natural frequency of brake system) [6] [7]. This is characteristic of the pattern formation phenomenon. It has been reported that hot judder occurs in the rotation frequency around 40 Hz. In Fig. 6, when the rotation speed is 41.39 Hz, the real part of the characteristic root of 10 hot spots is the maximum. In this case, hot judder occurs at 413.9 Hz. The unstable vibration frequency is almost identical to the second natural frequency 400 Hz in Table 3. Then, the complex mode for the unstable vibration obtained at rotation speed 41.39 Hz for 10 hot spots is shown in Table 4. The caliper of the inner side and the outer side vibrate approximately at the same amplitude and phase, and the disc vibrates with small amplitude and out-of-phase to the caliper, as shown in Table 4. In addition, the complex mode of the unstable vibration is the same as the second natural mode, and the quantity of the expansion of the inner side $u_i(t)$ and the quantity of the expansion of the outer side $u_o(t)$ have the same amplitude and are out of phase with each other. The difference of the amplitude ratios of $u_i(t)$ and $u_o(t)$ is related to the relative amplitude ratios $x_1$-$x_3$ and $x_2$-$x_3$. These complex modes of unstable vibration for the other numbers of hot spots located at different rotation speeds have the same vibration modes as that for 10 hot spots. In this calculation, unstable vibration of the first mode does not occur. The variation of the contact force in the first mode is smaller than that of the second mode. This is the reason why only the second mode becomes unstable.

Furthermore, the parameters of the coefficient of friction $\mu$, pad contact pressure $F$, disc angular velocity $\omega$ are very effective to the real parts of the characteristic roots in Fig. 6 because the heat flux quantity $\dot{q}_{in}$ in Eq. (2) is increased by these parameters and the disc temperature, and the quantity of disc expansions are increased.

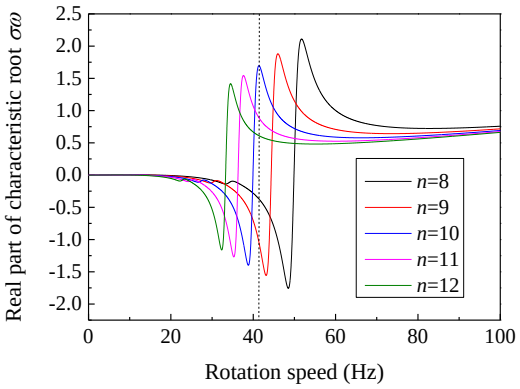


Fig. 6 Relation between real part $\sigma\omega$ and rotation speed

Table 4 Complex mode

| | Amplitude ratio | Phase (degree) |
|---|---|---|
| $x_1$ | 1.0 | 0 |
| $x_2$ | 0.8520 | 0.65 |
| $x_3$ | 0.06629 | -177 |
| $u_i$ | 0.1336 | -223.8 |
| $u_o$ | 0.1151 | -43.1 |

### 3.4 Simulation analysis result

The numerical integral calculation using the Runge-Kutta-Gill (RKG) method was performed on Eq. (10) through Eq. (14). A simulation is conducted under the condition of 41.39 Hz rotation speed and 10 hot spots, as shown by the vertical dotted line in Fig. 6. Figure 7 shows the vibration waveform of $x_1$. Figure 8 shows the frequency analysis for the waveform between 9 s and 10 s in Fig. 7.

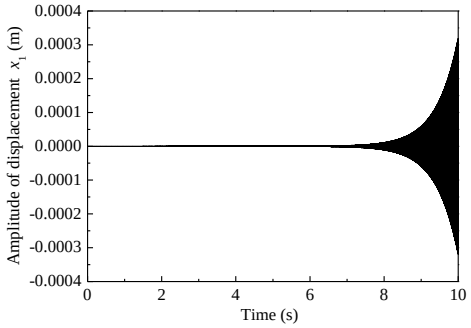


Fig. 7 Time-axis waveform of the amplitude of inner caliper $x_1$

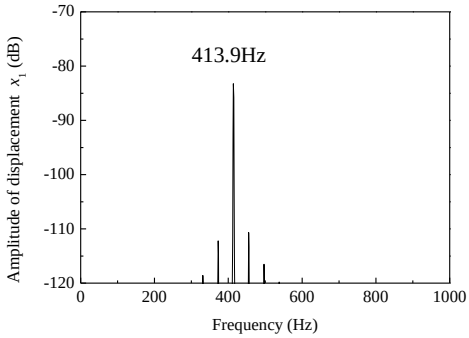


Fig. 8 Frequency analysis of the waveform

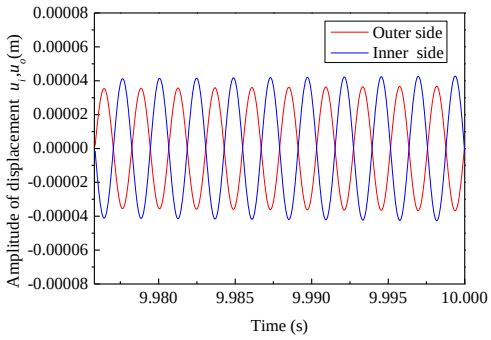


Fig. 9 Relation between expansion of the disc and time

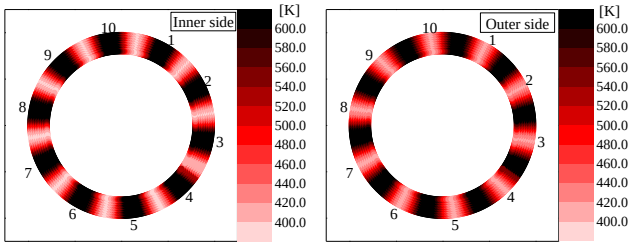


Fig. 10 Temperature of the disc on the inner side and outer side

From the calculation results, the frequency component of the generation frequency of hot judder is confirmed to be 413.9 Hz, which is close to the second natural frequency of the system.

Figure 9 shows the quantity of expansions of inner side $u_i$ and outer side $u_o$ for one revolution period. In Fig. 9, it is confirmed that the quantity of expansion fluctuates out of phase with the inner and outer sides.

Figure 10 shows the temperature distributions on the inner and outer sides of the disc when the operation time is in the same range shown in Fig. 9. In Fig. 10, 10 hot spots on the disc surface are confirmed. In addition, the large quantity of expansion increases temperature, and the maximum temperature reaches more than 600 K for ten seconds. The hot spots occur where the disc expansion is the largest, and these hot spots cause the hot judder of the caliper.

## 4. Conclusions

In this study, the generation mechanism of hot judder caused by thermal deformation in disc brakes was clarified. This paper concludes the following:

(1) The fluctuation of the contact force between the disc and pad due to vibration of the brake system causes fluctuation of the disc surface temperature, and fluctuation of the temperature causes larger fluctuation of the contact force in one rotation of the disc with time delay. It is concluded that hot spots and hot judder are excited by self-excited vibration with time delay.

(2) Only the second mode of the system becomes unstable. The generation frequency of hot judder is close to the second natural frequency of the brake system.
(3) The range of rotation speeds that cause the instability is large for each number of hot spots.
(4) Hot judder with 10 hot spots was reproduced as the simulation result.

## ACKNOWLEDGEMENT

The present study was supported in part by JSPS KAKENHI Grant Number 16K18042.

## REFERENCES

1 Masahiro Kubota, Tomihiro Suenaga, Kazuhiro Doi, *Development of a Method for Reducing Brake Judder*, Proceedings. JSAE Annual Congress, 972, pp1-4

2 J.R.BARBER, *Thermoelastic instabilities in the sliding of conforming solids*, The Royal Society, A. 312, 381-394 (1969)

3 Toshio Aihara, *HEAT TRANSFER*, SHOKABO, pp9, p180, p268, p272.

4 Kurasako Ryoichi, *Study for the Factors of Fluctuating Brake Friction Force*, Transactions of the Japan society of mechanical engineers series C, 78-786(2012-2), pp462-473.

5 Japan Society of Mechanical Engineers, JSME heat transfer handbook, pp57-58.

6 Sueoka Atsuo, Ryu Takahiro, Kondou Takahiro, Tsuda Yoshihiko, Katayama Keiichi, Takasaki Katsuaki, Yamaguchi Masahiro, Hirooka Hideki, Polygonal Deformation of Roll-Covering Rubber, Transactions of the Japan society of mechanical engineers, 92-1695, C(1993), 2078-2085.

7 Sueoka Atsuo, Ryu Takahiro, Kondou Takahiro, Togashi Minoru, Fujimoto Toshio, Polygonal Wear of Automobile Tires, Transactions of the Japan society of mechanical engineers, 96-0029, C(1996), 3145-3152.